# Heavy-fermion state in the Anderson lattice

T. Koyama and M. Tachiki
*The Research Institute for Iron, Steel and Other Metals, Tohoku University, Katahira 2-1-1, Sendai, Japan*
(Received 6 March 1986)

To investigate theoretically the heavy-fermion state in cerium and uranium compounds, the low-energy excited states in an Anderson lattice are studied at absolute zero. The coupled Dyson equations for both the Green's functions of the $f$ electron and the spin fluctuations are set up in the case of the finite correlation interaction energy. The vertex functions are approximately determined to fulfill the Ward-Takahashi relations which originate from the spin-rotational invariance, in the low-energy region. In the spectral density of the $f$-electron Green's function which is numerically calculated, it is found that a sharp peak corresponding to the state of quasifermions with heavy masses appears near the Fermi level, and a broad peak similar to the resonance peak in Kondo impurity systems appears in a relatively-high-energy region. As the temperature increases, the quasifermion peak diminishes and changes to the resonance peak.

## I. INTRODUCTION

Both cerium and uranium compounds have attracted much attention because of their unusual properties. Some of these compounds have extremely large coefficients of specific heat at low tempertures and are called the heavy-fermion compounds.[1] If cerium ions in the heavy fermion compounds such as $CeCu_6$ are replaced by lanthanum ions, the coefficient of specific heat becomes smaller and comparable to those of usual metals. This fact indicates that the $f$ electrons of cerium ions are responsible for the large coefficients of specific heat in the compounds. When temperature is relatively high, the electrical resistivity in typical heavy fermion compounds increases with decreasing temperature in a manner similar to that in Kondo impurity systems. As temperature further decreases, the resistivity attains a maximum at a certain temperature and then decreases. At low temperature, the resistivity is proportional to the square of temperature. This behavior at low temperatures is very different from that in Kondo impurity systems, in which the resistivity has the large value of unitarity limit. In this low-temperature region, the coefficient of specific heat is extremely large and it has a maximum at some temperature in compounds such as $CeCu_6$,[2,3] $CeAl_3$,[4] and $CeCu_2Si_2$.[5] This temperature is much lower than the temperature at which the resistivity has a maximum. Let us call this low-temperature state characteristic in these compounds the heavy-fermion state. The central problem in the heavy-fermion system is to understand the nature of the heavy-fermion state, and the crossover between this heavy-fermion state and the impuritylike state at high temperatures.

A model appropriate for treating the heavy-fermion system may be an Anderson-lattice model. In this model, the $f$-electron ions whose $f$-electron energy levels are inside the conduction band are regularly placed at all the lattice sites. The conduction electrons and the $f$ electrons are mixed by the mixing interaction. The strong correlation interaction acts between $f$ electrons when two $f$ electrons sit on the same site. Many theoreticians expected the existence of a narrow renormalized band of quasifermions near the Fermi level in the Anderson lattice. They used the following various methods for calculating the renormalized band: a single-site approximation for the self-energy of the $f$ electron,[6–8] the Korringa-Kohn-Rostoker (KKR) calculation by using the Nozières Fermi-liquid theory of the Kondo impurity,[9,10] the boson theory,[11–13] variational calculations,[14–16] and others.[17–22] In spite of their great efforts, it seems that these approaches, including ours, are not satisfactory. Therefore, in the present paper we try to attack the Anderson-lattice problem in a rather orthodox way. The Green's functions for the $f$ and conduction electrons contain the self-energy of the $f$ electron which originates from the correlation interaction between the $f$ electrons. We consider that the spin fluctuations dominantly contribute to the self-energy in a system in which the $f$-electron energy levels are placed deeply below the Fermi level. Then we set up the coupled Dyson equations for both the Green's functions of the $f$ electron and the spin fluctuations in the case of the finite correlation interaction energy. Between the self-energy and the vertex functions there are Ward-Takahashi relations which originate from the spin-rotational invariance. The vertex functions are approximately determined so as to fulfill the Ward-Takahashi relations in the low-energy region. We numerically solved the Dyson equations which are expressed by the coupled integral equations. The numerical results for the spectral density of the $f$-electron Green's function are as follows. When the wave number is fixed and the energy is changed, a very sharp peak appears near the Fermi level, corresponding to the quasifermion state. The energy dispersion of the quasifermion is very weak. This fact indicates that the effective mass of the fermion is very heavy. The quasifermions with the heavy mass may be responsible for the large coefficient of specific heat at low temperatures. Along with the sharp peak, a broad peak appears in a relatively high-energy region. This broad peak corresponds to the resonance peak which is similar

 

to the resonance peak in Kondo-impurity systems. The appearance of the quasifermion and resonance peaks near the Fermi level mentioned above is the characteristic feature in the heavy-fermion state. Although our calculation in the present paper is restricted at 0 K, we can infer the occurrence of the crossover between the heavy-fermion state and the impuritylike state at a finite temperature. The appearance of the quasifermion peak of the spectral density of 0 K is due to the fact that the imaginary part of the self-energy is extremely small at the pole of the Green's function appearing near the Fermi level. When temperature increases, the quasifermion peak diminishes since the imaginary part increases. Above a certain temperature the imaginary part becomes considerably large, and the quasifermion peak changes to the resonance peak. This change leads to the occurrence of the crossover from the heavy-fermion state to the impuritylike state when temperature increases.

In Sec. II we give the formulation for deriving the self-energy, the spin fluctuations, and the vertex functions for the Anderson lattice. In Sec. III we describe the procedure of the numerical calculation and present the results of the numerical calculations for the spectral densities of the Green's functions for the $f$ electron and the spin fluctuations. In Sec. IV we give discussions and summary.

## II. FORMULATION

We consider an Anderson lattice in which conduction electrons ($s$ electrons) and strongly correlated electrons ($f$ electrons) are coupled through a mixing interaction. We denote the field operators for the $s$ and $f$ electrons with spin $\sigma$, respectively, by $\psi_\sigma(x)$ and $\phi_\sigma(x)$. The Hamiltonian is then expressed as

$$H=\sum_\sigma \int d^3x\{\psi_\sigma^\dagger(x)\varepsilon(-\nabla^2)\psi_\sigma(x)+E_0\phi_\sigma^\dagger(x)\phi_\sigma(x) +V[\psi_\sigma^\dagger(x)\phi_\sigma(x)+\phi_\sigma^\dagger(x)\psi_\sigma(x)] +\tfrac{1}{2}U\phi_\sigma^\dagger(x)\phi_{-\sigma}^\dagger(x)\phi_{-\sigma}(x)\phi_\sigma(x)\} , \quad (2.1)$$

with

$$\varepsilon(-\nabla^2)=-\frac{1}{2m}\nabla^2-\mu . \quad (2.2)$$

Here, $E_0$ is the atomic $f$-electron level measured from the chemical potential $\mu$, $V$ is the mixing parameter, and $U$ is the correlation energy. This Hamiltonian gives the following equations for $\psi_\sigma(x)$ and $\phi_\sigma(x)$:

$$[i\partial_t-\varepsilon(-\nabla^2)]\psi_\sigma(x)=V\phi_\sigma(x) , \quad (2.3)$$

$$(i\partial_t-E_0)\phi_\sigma(x)=V\psi_\sigma(x)+U\phi_{-\sigma}^\dagger(x)\phi_{-\sigma}(x)\phi_\sigma(x) . \quad (2.4)$$

Let us introduce an $f$-electron causal Green's function defined by

$$g_\sigma(x-y)\equiv\langle\phi_\sigma(x)\phi_\sigma^\dagger(y)\rangle =\frac{i}{(2\pi)^4}\int d^4p\, g_\sigma(p)e^{ip(x-y)} , \quad (2.5)$$

where $p$ is the four-dimensional vector $(p_0,\mathbf{p})$. The equation for $g_\sigma(x-y)$ can be obtained by using Eqs. (2.3) and (2.4) as

$$\{i\partial_t-E_0-V^2/[i\partial_t-\varepsilon(-\nabla^2)]\}g_\sigma(x-y) =i\delta^{(4)}(x-y)+U\langle\phi_{-\sigma}^\dagger(x)\phi_{-\sigma}(x)\phi_\sigma(x)\phi_\sigma^\dagger(y)\rangle . \quad (2.6)$$

Using the self-energy function $\Sigma_\sigma(p)$ defined by the relation

$$U\langle\phi_{-\sigma}^\dagger(x)\phi_{-\sigma}(x)\phi_\sigma(x)\phi_\sigma^\dagger(y)\rangle =\frac{i}{(2\pi)^4}\int d^4p\,\Sigma_\sigma(p)g_\sigma(p)\exp[ip(x-y)] , \quad (2.7)$$

we find

$$g_\sigma(p)=1/[p_0-E_0-V^2/(p_0-\varepsilon_{\mathbf{p}})-\Sigma_\sigma(p)] , \quad (2.8)$$

where

$$\varepsilon_{\mathbf{p}}=\mathbf{p}^2/2m-\mu . \quad (2.9)$$

To construct the Dyson equation for $\Sigma_\sigma(p)$, we rewrite the two-particle Green's function on the right-hand side of Eq. (2.6) in a more convenient form. For this purpose we define a causal Green's function for the $f$-electron spin fluctuations and three-point functions as follows:

$$\Delta(x-y)=\langle\sigma_+(x)\sigma_-(y)\rangle=\frac{i}{(2\pi)^4}\int d^4q\,\Delta(q)\exp[iq(x-y)] , \quad (2.10)$$

$$\langle\sigma_+(x)\phi_\uparrow(x_1)\phi_\downarrow^\dagger(x_2)\rangle=\left[\frac{i}{(2\pi)^4}\right]^2\int d^4p\int d^4q[g_\uparrow(p)g_\downarrow(p+q)-\Delta(q)\Gamma_+(p;q;p+q)g_\uparrow(p)g_\downarrow(p+q)]e^{ipx_1+iqx-i(p+q)x_2} , \quad (2.11)$$

$$\langle\sigma_-(x)\phi_\downarrow(x_1)\phi_\uparrow^\dagger(x_2)\rangle=\left[\frac{i}{(2\pi)^4}\right]^2\int d^4p\int d^4q[g_\downarrow(p+q)g_\uparrow(p)-\Delta(q)\Gamma_-(p+q;q;p)g_\downarrow(p+q)g_\uparrow(p)]e^{i(p+q)x_1-iqx-ipx_2} , \quad (2.12)$$

where $\sigma_+(x)=\phi_\uparrow^\dagger(x)\phi_\downarrow(x)$ and $\sigma_-(x)=\phi_\downarrow^\dagger(x)\phi_\uparrow(x)$. In Eqs. (2.11) and (2.12) the electron spin fluctuation vertices $\Gamma_\pm(p;q;r)$ were introduced. The structure of the three-point functions is illustrated in Fig. 1. The two-particle Green's function in Eq. (2.6) is then rewritten in the form

$$\langle\phi_{-\sigma}^\dagger(x)\phi_{-\sigma}(x)\phi_\sigma(x)\phi_\sigma^\dagger(y)\rangle =\begin{cases}-\langle\sigma_-(x)\phi_\downarrow(x)\phi_\uparrow^\dagger(y)\rangle & \text{for } \sigma=\uparrow,\\ -\langle\sigma_+(x)\phi_\uparrow(x)\phi_\downarrow^\dagger(y)\rangle & \text{for } \sigma=\downarrow .\end{cases} \quad (2.13)$$

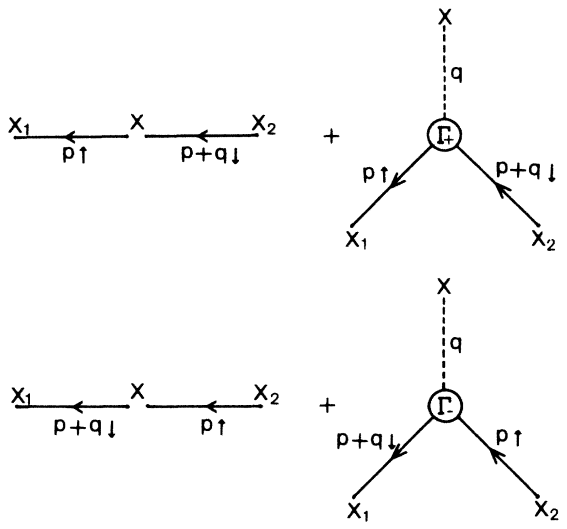


FIG. 1. Graphical representation of the three-point functions. (a) $\langle \sigma_+(x)\phi_\uparrow(x_1)\phi_\downarrow^\dagger(x_2)\rangle$, (b) $\langle \sigma_-(x)\phi_\downarrow(x_1)\phi_\uparrow^\dagger(x_2)\rangle$. The solid and broken lines represent, respectively, the Green's functions for the $f$ electron and the spin fluctuations.

Substituting Eqs. (2.11) and (2.12) into Eq. (2.13) and using the relation (2.7), we obtain the equation for the self-energy function,

$$\Sigma_\uparrow(p)=Un_\downarrow^f+U\frac{i}{(2\pi)^4}\int d^4q\,\Delta(q)\Gamma_-(p+q;q;p)\times g_\downarrow(p+q)\,, \tag{2.14}$$

$$\Sigma_\downarrow(p)=Un_\uparrow^f+U\frac{i}{(2\pi)^4}\int d^4q\,\Delta(q)\Gamma_+(p-q;q;p)\times g_\uparrow(p-q)\,, \tag{2.15}$$

where

$$n_{\uparrow,\downarrow}^f=-\frac{i}{(2\pi)^4}\int d^4p\,g_{\uparrow,\downarrow}(p)\,. \tag{2.16}$$

To solve Eqs. (2.14) and (2.15) we need equations for the spin-fluctuation Green's function and the vertex functions. The equation for $\Delta(q)$ can be obtained by observing

$$\langle \sigma_+(x)\sigma_-(y)\rangle=-\lim_{\tau\to 0+}\langle \sigma_+(x)\phi_\uparrow(t_y,\mathbf{y})\phi_\downarrow^+(t_y+\tau,\mathbf{y})\rangle\,. \tag{2.17}$$

Substituting Eqs. (2.10) and (2.11) into Eq. (2.17), we have the equation

$$\Delta(q)=-\frac{i}{(2\pi)^4}\int_c d^4p\,g_\uparrow(p)g_\downarrow(p+q)+\frac{i}{(2\pi)^4}\int_c d^4p\,\Delta(q)\Gamma_+(p;q;p+q)\times g_\uparrow(p)g_\downarrow(p+q)\,, \tag{2.18}$$

where the integration path $c$ is taken as $\mathrm{Im}p_0>0$. Equations (2.14), (2.15), and (2.18) provide a set of coupled equations to determine the $f$-electron self-energy and the spin-fluctuation Green's function if we have a knowledge about the vertex function $\Gamma_\pm(p\pm q;q;p)$. The graphical representation of the Dyson equations, (2.14), (2.15), and (2.18), is shown in Fig. 2.

Let us next study the vertex functions $\Gamma_\pm(p\pm q;q;p)$. The exact determination of the vertex functions is, in general, quite difficult and so we have to make a certain approximation for the vertex functions. The approximation we adopt is to replace the vertex functions in Eqs. (2.14) and (2.15) by a renormalized coupling constant $\lambda_r$ in the following way:

$$\Gamma_\pm(p\pm q;q;p)\simeq\Gamma_\pm(p_F;0;p_F)=\lambda_r \tag{2.19}$$

with $p_F=(0,\mathbf{p}_F)$.[23] In this case we have the following approximate equations for the self-energy:

$$\Sigma_\uparrow(p)=Un_\downarrow^f+\lambda_r^2\frac{i}{(2\pi)^4}\int d^4q\,g_\downarrow(p+q)\Delta(q)\,, \tag{2.20}$$

$$\Sigma_\downarrow(p)=Un_\uparrow^f+\lambda_r^2\frac{i}{(2\pi)^4}\int d^4q\,g_\uparrow(p-q)\Delta(q)\,. \tag{2.21}$$

Here we replaced also the bare coupling constant $U$ by the renormalized one, following the renormalization rule.[24] The above approximation corresponds to the one-loop approximation in which the self-energy diagram is composed of a loop formed by the spin-fluctuation and $f$-electron propagators. This type of approximation was successfully used in a formulation of itinerant electron ferromagnetism by Matsumoto *et al.*[25] As is well known in the theory of itinerant electron ferromagnetism, we must be careful of an approximation to the vertex function in the equation for the spin fluctuations.[25–28] For instance, the application of the approximation (2.19) to Eq. (2.18) along with the use of the self-energies (2.20) and (2.21) breaks the spin rotational invariance of the system. The rotational invariance plays an important role for the low-energy properties in magnetic systems, therefore we believe that a correct theory describing the heavy-fermion state of the Anderson lattice should not violate the spin rotational invariance of the system. For this reason, we seek an approximation to the vertex function in Eq. (2.18) which insures the spin rotational invariance. This can be

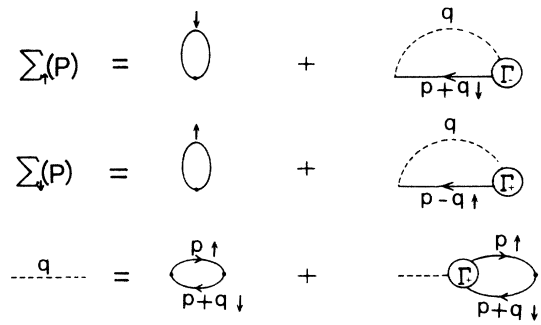


FIG. 2. Graphical representation of the equations for (a) the self-energy functions and (b) the spin-fluctuation Green's function.

achieved by using the Ward-Takahashi relations obtained from the spin rotational invariance of the system in the following way.

To derive the Ward-Takahashi relations we add the following symmetry-breaking terms to the Hamiltonian (2.1), since the Hamiltonian is invariant under the spin rotation for the $f$- and $s$-electron systems by the same angle,

$$-(h_s/2)\psi^\dagger(x)\sigma_3\psi(x)-(h_f/2)\phi^\dagger(x)\sigma_3\phi(x)\ , \tag{2.22}$$

where $\sigma_3$ is the Pauli spin matrix. The terms are equivalent to the Zeeman term if the parameters $h_s$ and $h_f$ are taken to be an external magnetic field. In the presence of the term (2.22) the equation for the three-point function (2.11) can be obtained as follows:

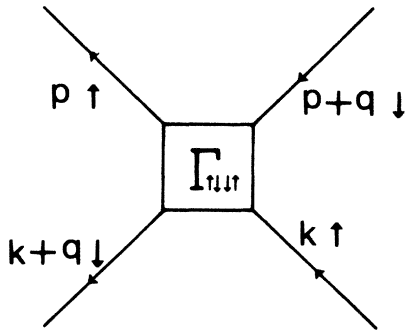


FIG. 3. Graphical representation of the vertex function $\Gamma_{\uparrow\downarrow,\downarrow\uparrow}(p,k+q;p+q,k)$.

$$(-i\partial_t+h_f)\langle\sigma_+(x)\phi_\uparrow(x_1)\phi_\downarrow^\dagger(x_2)\rangle=i\delta^{(4)}(x-x_1)g_\downarrow(x_1-x_2)-i\delta^{(4)}(x-x_2)g_\uparrow(x_1-x_2)$$
$$-V\langle[\phi_\uparrow^\dagger(x)\psi_\downarrow(x)-\psi_\uparrow^\dagger(x)\phi_\downarrow(x)]\phi_\uparrow(x_1)\phi_\downarrow^\dagger(x_2)\rangle\ . \tag{2.23}$$

Equation (2.23) leads to several useful Ward-Takahashi relations in our Anderson-lattice system. First we consider the case $x_1=x_2=y$. In this case we find, noting $g_{\uparrow,\downarrow}(0)=-n^f_{\uparrow,\downarrow}$, from (2.23),

$$-iM_f\delta^{(4)}(x-y)=(-i\partial_t+h_f)\langle\sigma_+(x)\sigma_-(y)\rangle+V\langle[\phi_\uparrow^\dagger(x)\psi_\downarrow(x)-\psi_\uparrow^\dagger(x)\phi_\downarrow(x)]\sigma_-(y)\rangle\ , \tag{2.24}$$

$M_f$ being the $f$-electron polarization,

$$M_f=n^f_\uparrow-n^f_\downarrow\ . \tag{2.25}$$

The three-point functions in Eq. (2.24) are rewritten as

$$\langle\phi_\uparrow^\dagger(x)\psi_\downarrow(x)\sigma_-(y)\rangle=-iV\int d^4z\,S_\downarrow(x-z)\langle\phi_\uparrow^\dagger(x)\phi_\downarrow(z)\sigma_-(y)\rangle\ , \tag{2.26}$$

$$\langle\psi_\uparrow^\dagger(x)\phi_\downarrow(x)\sigma_-(y)\rangle=-iV\int d^4z\,S_\uparrow(z-x)\langle\phi_\uparrow^\dagger(z)\phi_\downarrow(x)\sigma_-(y)\rangle\ , \tag{2.27}$$

where $S_\sigma(x-z)$ is the unperturbed conduction electron Green's function, i.e.,

$$S_\sigma(x)=i[i\partial_t-\varepsilon(-\nabla^2)+h_s\sigma_3/2]^{-1}\delta^{(4)}(x)\ . \tag{2.28}$$

Using Eqs. (2.26)–(2.28) and (2.12), we obtain the Fourier transformation of Eq. (2.24),

$$M_f=(q_0-h_f)\Delta(q)+V^2\frac{i}{(2\pi)^4}\int d^4p\frac{-q_0+h_s+\varepsilon_{p+q}-\varepsilon_p}{(p_0+q_0-\varepsilon_{p+q}-h_s/2)(p_0-\varepsilon_p+h_s/2)}g_\downarrow(p+q)g_\uparrow(p)$$
$$-V^2\frac{i}{(2\pi)^4}\int d^4p\frac{-q_0+h_s+\varepsilon_{p+q}-\varepsilon_p}{(p_0+q_0-\varepsilon_{p+q}-h_s/2)(p_0-\varepsilon_p+h_s/2)}g_\downarrow(p+q)g_\uparrow(p)\Gamma_-(p+q;q;p)\Delta(q)\ . \tag{2.29}$$

From this relation we have the following relation in the limit $q\to0$:

$$M_f=-h_f\chi_f+h_s\chi_s\ , \tag{2.30}$$

where

$$\chi_f=\Delta(0)\ , \tag{2.31}$$

$$\chi_s=V^2\frac{i}{(2\pi)^4}\int d^4p\frac{1}{(p_0-\varepsilon_p-h_s/2)(p_0-\varepsilon_p+h_s/2)}[1-\Delta(0)\Gamma_-(p;0;p)]g_\downarrow(p)g_\uparrow(p)\ . \tag{2.32}$$

Thus the magnetic susceptibility of the $f$-electron system is given by $(-\chi_f+\chi_s)$.

Let us next consider the Fourier transformation of Eq. (2.23). Unfortunately, the third term on the right-hand side of Eq. (2.23) cannot be expressed in terms of the electron spin-fluctuation vertex functions $\Gamma_\pm(p\pm q;q;p)$. Hence we introduce a vertex function with four $f$-electron external points $\Gamma_{\uparrow\downarrow,\downarrow\uparrow}$, which is illustrated in Fig. 3. The two-particle Green's function in Eq. (2.23) is then Fourier transformed as

$$\langle[\phi_\uparrow^\dagger(x)\psi_\downarrow(x)-\psi_\uparrow^\dagger(x)\phi_\downarrow(x)]\phi_\uparrow(x_1)\phi_\downarrow^\dagger(x_2)\rangle$$
$$=V\frac{i}{(2\pi)^4}\int d^4p\int d^4q\left[\frac{-q_0+h_s+\varepsilon_{p+q}-\varepsilon_p}{(p_0+q_0-\varepsilon_{p+q}-h_s/2)(p_0-\varepsilon_p+h_s/2)}g_\uparrow(p)g_\downarrow(p+q)\right.$$
$$+\frac{i}{(2\pi)^4}\int d^4k\frac{-q_0+h_s+\varepsilon_{k+q}-\varepsilon_k}{(k_0+q_0-\varepsilon_{k+q}-h_s/2)(k_0-\varepsilon_k+h_s/2)}$$
$$\left.\times g_\uparrow(p)g_\downarrow(k+q)\Gamma_{\uparrow\downarrow,\downarrow\uparrow}(p,k+q;p+q,k)g_\downarrow(p+q)g_\uparrow(k)\right]$$
$$\times\exp[ipx_1+iqx-i(p+q)x_2]\,. \tag{2.33}$$

Substituting Eq. (2.33) into Eq. (2.23), we can obtain the following equation after some calculations:

$$g_\uparrow^{-1}(p)-g_\downarrow^{-1}(p+q)=-(q_0-h_f)+(q_0-h_f)\Delta(q)\Gamma_+(p;q;p+q)+\frac{V^2(-q_0+h_s+\varepsilon_{p+q}-\varepsilon_p)}{(p_0+q_0-\varepsilon_{p+q}-h_s/2)(p_0-\varepsilon_p+h_s/2)}$$
$$+V^2\frac{i}{(2\pi)^4}\int d^4k\frac{-q_0+h_s+\varepsilon_{k+q}-\varepsilon_k}{(k_0+q_0-\varepsilon_{k+q}-h_s/2)(k_0-\varepsilon_k+h_s/2)}g_\downarrow(k+q)g_\uparrow(k)\Gamma_{\uparrow\downarrow,\downarrow\uparrow}(p,k+q;p+q;k)\,. \tag{2.34}$$

Since the $f$-electron Green's function is written as

$$g_{\uparrow,\downarrow}^{-1}(p)=p_0-E_0\pm h_f/2-V^2/(p_0-\varepsilon_p\pm h_s/2)-\Sigma_{\uparrow,\downarrow}(p)\,, \tag{2.35}$$

we can relate the vertex functions to the $f$-electron self-energy,

$$\Sigma_\downarrow(p+q)-\Sigma_\uparrow(p)=(q_0-h_f)\Delta(q)\Gamma_+(p;q;p+q)$$
$$+V^2\frac{i}{(2\pi)^4}\int d^4k\frac{-q_0+h_s+\varepsilon_{k+q}-\varepsilon_k}{(k_0+q_0-\varepsilon_{k+q}-h_s/2)(k_0-\varepsilon_k+h_s/2)}g_\downarrow(k+q)g_\uparrow(k)\Gamma_{\uparrow\downarrow,\downarrow\uparrow}(p,k+q;p+q,k)\,. \tag{2.36}$$

In the limit $q\to0$, Eq. (2.36) is reduced to

$$\Sigma_\downarrow(p)-\Sigma_\uparrow(p)=-h_f\Delta(0)\Gamma_+(p;0;p)$$
$$+h_s\frac{i}{(2\pi)^4}\int d^4k\frac{V^2}{(k_0-\varepsilon_k-h_s/2)(k_0-\varepsilon_k+h_s/2)}g_\downarrow(k)g_\uparrow(k)\Gamma_{\uparrow\downarrow,\downarrow\uparrow}(p,k;p,k)\,. \tag{2.37}$$

When only linear terms with respect to $h_f$ and $h_s$ are retained, we find from (2.37)

$$\Sigma_\downarrow(p)-\Sigma_\uparrow(p)=-2h_f\left[\frac{\partial\Sigma_\uparrow(p)}{\partial h_f}\right]_{h=0}-2h_s\left[\frac{\partial\Sigma_\uparrow(p)}{\partial h_s}\right]_{h=0}$$
$$=-h_f\Delta(0)\Gamma_+(p;0;p)+h_s\frac{i}{(2\pi)^4}\int d^4k\frac{V^2}{(k_0-\varepsilon_k)^2}g_\downarrow(k)g_\uparrow(k)\Gamma_{\uparrow\downarrow,\downarrow\uparrow}(p,k;p,k)\,. \tag{2.38}$$

This equation indicates the following relations:

$$\left[\frac{\partial\Sigma_\uparrow(p)}{\partial h_f}\right]_{h=0}=\tfrac{1}{2}\Delta(0)\Gamma_+(p;0;p)\,, \tag{2.39}$$

$$\left[\frac{\partial\Sigma_\uparrow(p)}{\partial h_s}\right]_{h=0}=-\tfrac{1}{2}\frac{i}{(2\pi)^4}\int d^4k\frac{V^2}{(k_0-\varepsilon_k)^2}g_\downarrow(k)g_\uparrow(k)\Gamma_{\uparrow\downarrow,\downarrow\uparrow}(p,k;p,k)\,. \tag{2.40}$$

These relations are the Ward-Takahashi relations resulting from the spin rotational invariance of the Anderson-lattice system.[29] Furthermore, noting the relation in the case $q\to0$,

$$\Sigma_\downarrow(p+q)-\Sigma_\uparrow(p)=[\Sigma_\downarrow(p+q)-\Sigma_\downarrow(p)]+[\Sigma_\downarrow(p)-\Sigma_\uparrow(p)]$$
$$\simeq q_0\left[\frac{\partial\Sigma_\downarrow(p)}{\partial p_0}\right]+\mathbf{q}\cdot\frac{\partial\Sigma_\downarrow(p)}{\partial\mathbf{p}}+[\Sigma_\downarrow(p)-\Sigma_\uparrow(p)]\,, \tag{2.41}$$

we also have the Ward-Takahashi relations from Eq. (2.36) in the limit of $h_f$ and $h_s \to 0$,

$$\left[\frac{\partial\Sigma_\downarrow(p)}{\partial p_0}\right]_{h=0} = \Delta(0)\Gamma_+(p;0;p) - \frac{i}{(2\pi)^4}\int d^4k \frac{V^2}{(k_0-\varepsilon_k)^2} g_\downarrow(k)g_\uparrow(k)\Gamma_{\uparrow\downarrow,\downarrow\uparrow}(p,k;p,k)$$
$$= 2\left[\frac{\partial\Sigma_\uparrow(p)}{\partial h_f}\right]_{h=0} + 2\left[\frac{\partial\Sigma_\uparrow(p)}{\partial h_s}\right]_{h=0}, \tag{2.42}$$

$$\left[\frac{\partial\Sigma_\downarrow(p)}{\partial \mathbf{p}}\right]_{h=0} = \frac{i}{(2\pi)^4}\int d^4k \frac{V^2}{(k_0-\varepsilon_k)^2}\frac{\partial\varepsilon_k}{\partial \mathbf{k}} g_\downarrow(k)g_\uparrow(k)\Gamma_{\uparrow\downarrow,\downarrow\uparrow}(p,k;p,k)\,. \tag{2.43}$$

Since these relations are the manifestation of the rotational invariance of the system, we can make use of the relations as a guiding principle for solving approximately Eq. (2.34) for $\Gamma_+(p;q;p+q)$.

The approximation we adopt in solving Eq. (2.34) is to replace the last term on the right-hand side of (2.34) by the expression in its small $q$ limit, i.e.,

$$V^2\frac{i}{(2\pi)^4}\int d^4k \frac{-q_0+h_s+\varepsilon_{k+q}-\varepsilon_k}{(k_0+q_0-\varepsilon_{k+q})(k_0-\varepsilon_k)} g_\downarrow(k+q)g_\uparrow(k)\Gamma_{\uparrow\downarrow,\downarrow\uparrow}(p,k+q;p+q,k)$$
$$\simeq(-q_0+h_s)\frac{i}{(2\pi)^4}\int d^4k\frac{V^2}{(k_0-\varepsilon_k)^2} g_\downarrow(k)g_\uparrow(k)\Gamma_{\uparrow\downarrow,\downarrow\uparrow}(p,k;p,k)$$
$$+\mathbf{q}\cdot\frac{i}{(2\pi)^4}\int d^4k\frac{V^2}{(k_0-\varepsilon_k)^2}\frac{\partial\varepsilon_k}{\partial\mathbf{k}} g_\downarrow(k)g_\uparrow(k)\Gamma_{\uparrow\downarrow,\downarrow\uparrow}(p,k;p,k)$$
$$=2(q_0-h_s)\left[\frac{\partial\Sigma_\uparrow(p)}{\partial h_s}\right]_{h=0} + \mathbf{q}\cdot\left[\frac{\partial\Sigma_\downarrow(p)}{\partial\mathbf{p}}\right]_{h=0}. \tag{2.44}$$

Here we assumed $h_s \simeq 0$. Substituting Eq. (2.44) into Eq. (2.34), we obtain the approximate vertex function $\Gamma_+(p;q;p+q)$ in terms of the self-energy,

$$(q_0-h_f)\Delta(q)\Gamma_+(p;q;p+q) \simeq g_\uparrow^{-1}(p) - g_\downarrow^{-1}(p+q) + (q_0-h_f) - \frac{V^2(-q_0+h_s+\varepsilon_{p+q}-\varepsilon_p)}{(p_0+q_0-\varepsilon_{p+q}-h_s/2)(p_0-\varepsilon_p+h_s/2)}$$
$$-2(q_0-h_s)\left[\frac{\partial\Sigma_\uparrow(p)}{\partial h_s}\right]_{h=0} - \mathbf{q}\cdot\left[\frac{\partial\Sigma_\downarrow(p)}{\partial\mathbf{p}}\right]_{h=0}. \tag{2.45}$$

The relation, of course, is compatible with the Ward-Takahashi relations (2.39), (2.40), (2.42), and (2.43), as can easily be checked.

The equation for the spin-fluctuation Green's function (2.18) can be rewritten in the form consistent with the equation for the self-energy (2.20) and (2.21) by making use of (2.45). To do this, we rewrite Eq. (2.18) in the following form:

$$(q_0-h_f)\Delta(q) = -(q_0-h_f)\frac{i}{(2\pi)^4}\int_c d^4p\, g_\uparrow(p)g_\downarrow(p+q) + \frac{i}{(2\pi)^4}\int_c d^4p\, g_\uparrow(p)g_\downarrow(p+q)$$
$$\times(q_0-h_f)\Delta(q)\Gamma_+(p;q;p+q)\,. \tag{2.46}$$

Then, substituting (2.45) into (2.46), we obtain the equation in the limit of $h_s$, $h_f \to 0$ as

$$q_0\Delta(q) = -V^2\frac{i}{(2\pi)^4}\int_c d^4p \frac{-q_0+\varepsilon_{p+q}-\varepsilon_p}{(p_0+q_0-\varepsilon_{p+q})(p_0-\varepsilon_p)} g_\uparrow(p)g_\downarrow(p+q)$$
$$-2q_0\frac{i}{(2\pi)^4}\int_c d^4p\, g_\uparrow(p)\left[\frac{\partial\Sigma_\uparrow(p)}{\partial h_s}\right]_{h=0} g_\downarrow(p+q) - \mathbf{q}\cdot\frac{i}{(2\pi)^4}\int_c d^4p\, g_\uparrow(p)\left[\frac{\partial\Sigma_\downarrow(p)}{\partial\mathbf{p}}\right]_{h=0} g_\downarrow(p+q)\,. \tag{2.47}$$

Along with Eq. (2.20) or Eq. (2.21) this equation provides a set of coupled equations to determine the self-energy and the spin-fluctuation Green's function self-consistently. The renormalized coupling constant $\lambda r$ in Eq. (2.20) or Eq. (2.21) is given by the relation (2.39) at $p = p_F$.

## III. NUMERICAL CALCULATION

In this section we illustrate how to solve Eqs. (2.20), (2.21), and (2.47). To procure the self-consistent solution, we will try to make an iterative calculation. In the present paper we obtain the lowest-order solution in the

iterative calculation.

First we rewrite the equations for the self-energy and the spin fluctuations in a more convenient form for the numerical calculations, using the spectral representation for $g_\sigma(p)$ and $\Delta(q)$

$$g_\sigma(p)=\int dw\,\rho_\sigma(w,\mathbf{p})\left[\frac{\Theta(w)}{p_0-w+i\delta}+\frac{\Theta(-w)}{p_0-w-i\delta}\right], \tag{3.1}$$

$$\Delta(q)=\int dw\,D(w,\mathbf{q})\left[\frac{\Theta(w)}{q_\sigma-w+i\delta}+\frac{\Theta(-w)}{q_0-w-i\delta}\right], \tag{3.2}$$

where $\rho_\sigma(w,\mathbf{p})$ and $D(w,\mathbf{q})$ are the spectral functions, $\Theta(w)$ is the step function, and $\delta$ is an infinitesimal positive number. Substitution of Eqs. (3.1) and (3.2) into Eqs. (2.20) and (2.21) leads to

$$\Sigma_\uparrow(p)=Un^f_\downarrow+\int dw\,\tilde{\Sigma}_{2\uparrow}(w,\mathbf{p})\times\left[\frac{\Theta(w)}{p_0-w+i\delta}+\frac{\Theta(-w)}{p_0-w-i\delta}\right], \tag{3.3}$$

$$\Sigma_\downarrow(p)=Un^f_\uparrow+\int dw\,\tilde{\Sigma}_{2\downarrow}(w,\mathbf{p})\times\left[\frac{\Theta(w)}{p_0-w+i\delta}+\frac{\Theta(-w)}{p_0-w-i\delta}\right], \tag{3.4}$$

where

$$\tilde{\Sigma}_{2\uparrow}(w,\mathbf{p})=\lambda_r^2\int dq_0\int\frac{d^3q}{(2\pi)^3}\rho_\downarrow(w+q_0,\mathbf{p}+\mathbf{q})\times D(q_0,\mathbf{q})[\Theta(q_0)-\Theta(q_0+w)], \tag{3.5}$$

$$\tilde{\Sigma}_{2\downarrow}(w,\mathbf{p})=\lambda_r^2\int dq_0\int\frac{d^3q}{(2\pi)^3}\rho_\uparrow(w-q_0,\mathbf{p}-\mathbf{q})\times D(q_0,\mathbf{q})[\Theta(q_0)-\Theta(q_0-w)]. \tag{3.6}$$

In zero field the self-energy does not depend on the spin direction, so we use Eq. (3.3) in which the spin index is dropped. As noted from the Green's function (2.8), the bare $f$ level $E_0$ always appears in combination with the self-energy in the form $E_0+\Sigma(p)$. We divide the combination as follows:

$$E_0+\Sigma(p)=\tilde{E}_0+\tilde{\Sigma}(p), \tag{3.7}$$

where

$$\tilde{E}_0\equiv E_0+\Sigma(0,\mathbf{p}_F), \tag{3.8}$$

$$\tilde{\Sigma}(p)\equiv\Sigma(p)-\Sigma(0,\mathbf{p}_F). \tag{3.9}$$

Here $\mathbf{p}_F$ is the Fermi momentum which will be defined later. Using (3.3), we have

$$\mathrm{Re}\tilde{\Sigma}(p)=\tilde{\Sigma}_1(p)=\int dw\left[\frac{\tilde{\Sigma}_2(w,\mathbf{p})}{p_0-w}+\frac{\tilde{\Sigma}_2(0,\mathbf{p}_F)}{w}\right], \tag{3.10}$$

$$\mathrm{Im}\Sigma(p)=-\pi\tilde{\Sigma}_2(p_0,\mathbf{p})\mathrm{sgn}(p_0). \tag{3.11}$$

The lowest-order approximation is employed in the following calculations. First we approximate the spectral function $\rho(w,\mathbf{p})$ in (3.5) in the form

$$\rho(w,\mathbf{p})\sim\rho_0(w,\mathbf{p})=\delta(w-\tilde{E}_0-V^2/(w-\varepsilon_\mathbf{p})). \tag{3.12}$$

This expression corresponds to the Hartree-Fock spectral function with the renormalized $f$ level, $\tilde{E}_0$. The spectral function of the spin-fluctuation Green's function, $D(q_0,\mathbf{q})$, in (3.5) is calculated in this approximation as follows. As seen from the equation for the spin fluctuations (2.47), we have to estimate the derivatives of the self-energy. When the spectral function (3.12) is used, they are given by

$$\left[\frac{\partial\Sigma_\uparrow(p)}{\partial h_s}\right]_{h=0}=U(\partial n_\downarrow/\partial h_s)_{h=0}=-U\chi_s/2, \tag{3.13}$$

$$\left[\frac{\partial\Sigma_\uparrow(p)}{\partial\mathbf{p}}\right]_{h=0}=0. \tag{3.14}$$

In deriving Eq. (3.13) the relation (2.30) was used. Substituting Eqs. (3.13) and (3.14) into Eq. (2.47), we obtain

$$q_0\Delta(q)=-P(q)+U\chi_s q_0 Q(p), \tag{3.15}$$

with

$$P(q)=V^2\frac{i}{(2\pi)^4}\int_c d^4p\frac{-q_0+\varepsilon_{\mathbf{p}+\mathbf{q}}-\varepsilon_\mathbf{p}}{(p_0+q_0-\varepsilon_{\mathbf{p}+\mathbf{q}})(p_0-\varepsilon_\mathbf{p})}\times g_\uparrow(p)g_\downarrow(p+q), \tag{3.16}$$

and

$$Q(q)=\frac{i}{(2\pi)^4}\int_c d^4p\,g_\uparrow(p)g_\downarrow(p+q). \tag{3.17}$$

$P(q)$ and $Q(q)$ can be rewritten by using the spectral representation (3.1) as

$$P(q)=V^2\int dw\int dp_0\int\frac{d^3p}{(2\pi)^3}\frac{-w+\varepsilon_{\mathbf{p}+\mathbf{q}}-\varepsilon_\mathbf{p}}{(p_0+w-\varepsilon_{\mathbf{p}+\mathbf{q}})(p_0-\varepsilon_\mathbf{p})}\rho_0(p_0,\mathbf{p})\times\rho_0(p_0+w,\mathbf{p}+\mathbf{q})[\Theta(p_0)-\Theta(p_0+w)]\left[\frac{\Theta(w)}{q_0-w+i\delta}+\frac{\Theta(-w)}{q_0-w-i\delta}\right], \tag{3.18}$$

$$Q(q)=\int dw\int dp_0\int\frac{d^3p}{(2\pi)^3}\rho_0(p_0,\mathbf{p})\rho_0(p_0+w,\mathbf{p}+\mathbf{q})[\Theta(p_0)-\Theta(p_0+w)]\left[\frac{\Theta(w)}{q_0-w+i\delta}+\frac{\Theta(-w)}{q_0-w-i\delta}\right]. \tag{3.19}$$

Thus the spectral function for the spin-fluctuation Green's function is obtained from Eqs. (3.15), (3.18), and (3.19) as

$$D(q_0,\mathbf{q})=\int dp_0 \int \frac{d^3p}{(2\pi)^3}\left[-\frac{V^2(-q_0+\varepsilon_{\mathbf{p}+\mathbf{q}}-\varepsilon_{\mathbf{p}})}{q_0(p_0+q_0-\varepsilon_{\mathbf{p}+\mathbf{q}})(p_0-\varepsilon_{\mathbf{p}})}+U\chi_s\right]\rho_0(p_0,\mathbf{p})\rho_0(p_0+q_0,\mathbf{p}+\mathbf{q})[\Theta(p_0)-\Theta(p_0+q_0)] . \quad (3.20)$$

Let us proceed to the calculation, using the spectral function (3.12). Since the spectral function (3.12) is rewritten as

$$\rho_0(p_0,\mathbf{p})=\frac{|p_0-\varepsilon_{\mathbf{p}}|}{B(\mathbf{p})}[\delta(p_0-A_+(\mathbf{p}))+\delta(p_0-A_-(\mathbf{p}))] , \quad (3.21)$$

where

$$A_\pm(\mathbf{p})=[(\tilde{E}_0+\varepsilon_{\mathbf{p}})\pm B(\mathbf{p})]/2 , \quad (3.22)$$

$$B(\mathbf{p})=[(\tilde{E}_0-\varepsilon_{\mathbf{p}})^2+4V^2]^{1/2} , \quad (3.23)$$

the integration by $p_0$ in (3.20) can be performed as follows:

$$D(q_0,\mathbf{q})=D_1(q_0,\mathbf{q})+D_2(q_0,\mathbf{q})+D_3(q_0,\mathbf{q})+D_4(q_0,\mathbf{q}) \quad (3.24)$$

where

$$D_1(q_0,\mathbf{q})=\pi\int\frac{d^3p}{(2\pi)^3}\frac{1}{B(\mathbf{p})B(\mathbf{p}+\mathbf{q})}(U\chi_s|A_+(\mathbf{p})-\varepsilon_{\mathbf{p}}||q_0+A_+(\mathbf{p})-\varepsilon_{\mathbf{p}+\mathbf{q}}|$$
$$-V^2(-q_0+\varepsilon_{\mathbf{p}+\mathbf{q}}-\varepsilon_{\mathbf{p}})\mathrm{sgn}\{[q_0+A_+(\mathbf{p})-\varepsilon_{\mathbf{p}+\mathbf{q}}][A_+(\mathbf{p})-\varepsilon_{\mathbf{p}}]\}/q_0)$$
$$\times\delta(q_0+A_+(\mathbf{p})-A_+(\mathbf{p}+\mathbf{q}))[\Theta(A_+(\mathbf{p}))-\Theta(q_0+A_+(\mathbf{p}))] , \quad (3.25)$$

$$D_2(q_0,\mathbf{q})=\pi\int\frac{d^3p}{(2\pi)^3}\frac{1}{B(\mathbf{p})B(\mathbf{p}+\mathbf{q})}(U\chi_s|A_+(\mathbf{p})-\varepsilon_{\mathbf{p}}||q_0+A_+(\mathbf{p})-\varepsilon_{\mathbf{p}+\mathbf{q}}|$$
$$-V^2(-q_0+\varepsilon_{\mathbf{p}+\mathbf{q}}-\varepsilon_{\mathbf{p}})\mathrm{sgn}\{[q_0+A_+(\mathbf{p})-\varepsilon_{\mathbf{p}+\mathbf{q}}][A_+(\mathbf{p})-\varepsilon_{\mathbf{p}}]\}/q_0)$$
$$\times\delta(q_0+A_+(\mathbf{p})-A_-(\mathbf{p}+\mathbf{q}))[\Theta(A_+(\mathbf{p}))-\Theta(q_0+A_+(\mathbf{p}))] , \quad (3.26)$$

$$D_3(q_0,\mathbf{q})=\pi\int\frac{d^3p}{(2\pi)^3}\frac{1}{B(\mathbf{p})B(\mathbf{p}+\mathbf{q})}(U\chi_s|A_-(\mathbf{p})-\varepsilon_{\mathbf{p}}||q_0+A_-(\mathbf{p})-\varepsilon_{\mathbf{p}+\mathbf{q}}|$$
$$-V^2(-q_0+\varepsilon_{\mathbf{p}+\mathbf{q}}-\varepsilon_{\mathbf{p}})\mathrm{sgn}\{[q_0+A_-(\mathbf{p})-\varepsilon_{\mathbf{p}+\mathbf{q}}][A_-(\mathbf{p})-\varepsilon_{\mathbf{p}}]\}/q_0)$$
$$\times\delta(q_0+A_-(\mathbf{p})-A_+(\mathbf{p}+\mathbf{q}))[\Theta(A_-(\mathbf{p}))-\Theta(q_0+A_-(\mathbf{p}))] , \quad (3.27)$$

$$D_4(q_0,\mathbf{q})=\pi\int\frac{d^3p}{(2\pi)^3}\frac{1}{B(\mathbf{p})B(\mathbf{p}+\mathbf{q})}(U\chi_s|A_-(\mathbf{p})-\varepsilon_{\mathbf{p}}||q_0+A_-(\mathbf{p})-\varepsilon_{\mathbf{p}+\mathbf{q}}|$$
$$-V^2(-q_0+\varepsilon_{\mathbf{p}+\mathbf{q}}-\varepsilon_{\mathbf{p}})\mathrm{sgn}\{[q_0+A_-(\mathbf{p})-\varepsilon_{\mathbf{p}+\mathbf{q}}][A_-(\mathbf{p})-\varepsilon_{\mathbf{p}}]\}/q_0)$$
$$\times\delta(q_0+A_-(\mathbf{p})-A_-(\mathbf{p}+\mathbf{q}))[\Theta(A_-(\mathbf{p}))-\Theta(q_0+A_-(\mathbf{p}))] . \quad (3.28)$$

To make the momentum integrations we rewrite the bare conduction-band energy as

$$\varepsilon_{\mathbf{p}}=\mathbf{p}^2/2m-\mu=\varepsilon_{\mathbf{p}_F}+\xi_p-\xi_{p_F} , \quad (3.29)$$

$$\varepsilon_{\mathbf{p}+\mathbf{q}}=\varepsilon_{\mathbf{p}_F}-\xi_{p_F}+\xi_p+2\xi_p^{1/2}\xi_q^{1/2}\cos\Theta+\xi_q , \quad (3.30)$$

where $\Theta$ is the angle between $\mathbf{p}$ and $\mathbf{q}$, and

$$\varepsilon_{\mathbf{p}_F}=\mathbf{p}_F^2/2m-\mu,\quad \xi_p=\mathbf{p}^2/2m . \quad (3.31)$$

Here the Fermi momentum $\mathbf{p}_F$ is given by the relation

$$\varepsilon_{\mathbf{p}_F}=V^2/\tilde{E}_0 . \quad (3.32)$$

This relation is obtained in the following way. The energy spectrum of our system is determined by the equation

$$p_0-\tilde{E}_0-V^2/[p_0-\varepsilon_{\mathbf{p}}]-\tilde{\Sigma}(p_0,\mathbf{p})=0 . \quad (3.33)$$

If the system is metallic, $p_0=0$ and $\mathbf{p}=\mathbf{p}_F$ must be a solution of Eq. (3.33), i.e.,

$$-\tilde{E}_0+V^2/\varepsilon_{\mathbf{p}_F}-\tilde{\Sigma}(0,\mathbf{p}_F)=0 . \quad (3.34)$$

This relation leads to the relation (3.32) because $\tilde{\Sigma}(0,\tilde{p}_F)=0$ owing to the definition (3.9). The integration

variable $\mathbf{p}$ in Eqs. (3.25)–(3.28) can be changed into the variables $\xi_p$ and $\Theta$. The results of integrations of Eqs. (3.25)–(3.28) and the imaginary part of the self-energy function $\Sigma_2(p_0,\xi_p)$ are given in the Appendix.

Since the $f$-electron Green's function is expressed in terms of $\Sigma_2(p_0,\xi_p)$, and $\Sigma_1(p_0,\xi_p)$ obtained from the integral (3.10) as

$$g(p)=1/[p_0-\tilde{E}_0-V^2/(p_0-\varepsilon_p)-\tilde{\Sigma}_1(p_0,\xi_p)+i\pi\tilde{\Sigma}_2(p_0,\xi_p)\mathrm{sgn}(p_0)]\ , \tag{3.35}$$

the spectral function of the $f$-electron Green's function can be calculated from the relation

$$\rho(p_0,\xi_p)=\frac{\tilde{\Sigma}_2(p_0,\xi_p)}{[p_0-\tilde{E}_0-V^2/(p_0-\varepsilon_p)-\tilde{\Sigma}_1(p_0,\xi_p)]^2+[\pi\tilde{\Sigma}_2(p_0,\xi_p)]^2}\ . \tag{3.36}$$

Now we present the numerical results for the low-energy properties of the Anderson lattice. The parameters which we use are $\tilde{E}_0/\xi_{p_F}$, $V/\xi_{p_F}$, $U\rho_s(\xi_{p_F})$, and $D/\xi_{p_F}$. First we choose the following values of the parameters, $\tilde{E}_0/\xi_{p_F}=-0.003$, $V/\xi_{p_F}=0.02$, $U\rho_s(\xi_{p_F})=0.1$, and $D/\xi_{p_F}=1.5$. In this choice we suppose the case $\xi_{p_F}\sim 10^4$ K, $|\tilde{E}_0|\sim 10K$, and $V\sim 10^2K$. In Fig. 4 the imaginary part of the spin-fluctuation Green's function is plotted as a function of the normalized energy $q_0/\xi_{p_F}$ for the various wave numbers $\xi_q/\xi_{p_F}$. As seen in this figure, a double peak structure is seen in the low-energy region. This structure originates from the two peaks in the $f$-electron spectral function which will be shown later. The wave-number dependence is very weak for the most part except the low-energy range. This means that the spin fluctuations in the $f$-electron system are almost localized on the lattice site. Figure 5 shows the energy dependence of the imaginary part of the $f$-electron self-energy function near the Fermi level $p_0=0$. The imaginary part of the self-energy vanishes at the Fermi level. Its energy dependence near the Fermi level is given by $\mathrm{Im}\Sigma(p_0,\mathbf{p})\propto p_0^2$. This result is easily obtained by considering Eq. (3.5) as follows. In the case of $p_0\sim 0$ Eq. (3.5) is expanded as

$$\tilde{\Sigma}_{2\uparrow}(p_0,\mathbf{p})\sim-\lambda_r^2\int\frac{d^3q}{(2\pi)^3}\rho_\downarrow(0,\mathbf{p}+\mathbf{q})D(0,\mathbf{q})p_0+\frac{\lambda_r^2}{2}\int\frac{d^3q}{(2\pi)^3}\frac{\partial}{\partial q_0}[\rho_\downarrow(q_0,\mathbf{p}+\mathbf{q})D(q_0,\mathbf{q})]\,|_{q_0=0}p_0^2+O(p_0^3)\ . \tag{3.37}$$

Since the spectral function of the $f$-electron spin fluctuations $D(q_0,\mathbf{q})$ linearly depends on $q_0$ in the low-energy region as seen from Eq. (3.20),

$$D(q_0,\mathbf{q})\sim\int\frac{d^3p}{(2\pi)^3}\left[U\chi_s-\frac{V^2(\varepsilon_{\mathbf{p}+\mathbf{q}}-\varepsilon_{\mathbf{p}})}{\varepsilon_{\mathbf{p}}\varepsilon_{\mathbf{p}+\mathbf{q}}}\right]\times\rho_0(0,\mathbf{p})\rho_0(0,\mathbf{p}+\mathbf{q})q_0+O(q_0)\ , \tag{3.38}$$

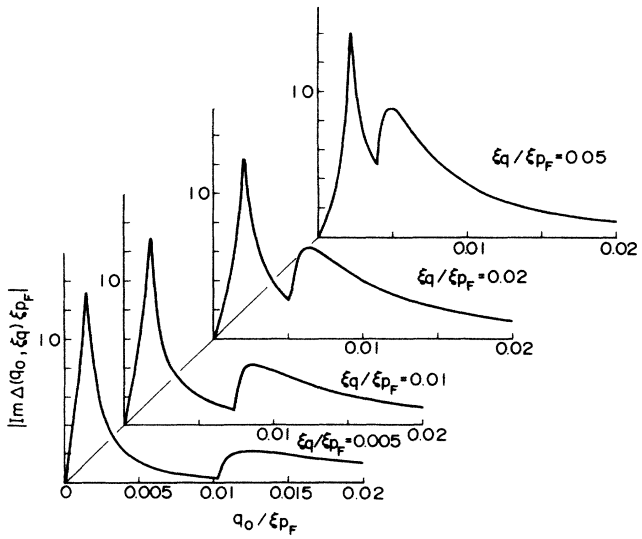


FIG. 4. Energy dependence of the imaginary part of the spin-fluctuation Green's function. The following values of the parameters are used: $\tilde{E}_0/\xi_{p_F}=-0.003$, $V/\xi_{p_F}=0.02$, $U\rho_s(\xi_{p_F})=0.1$, and $D/\xi_{p_F}=1.5$.

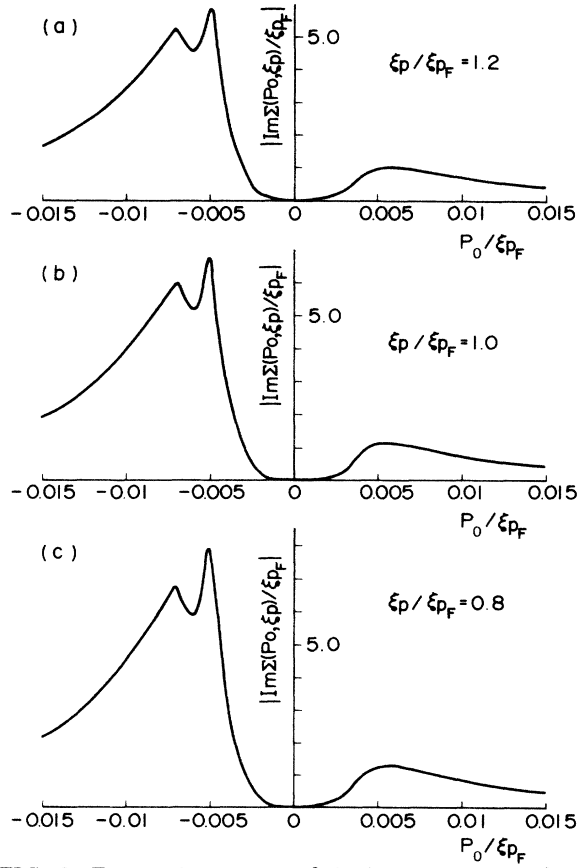


FIG. 5. Energy dependence of the imaginary part of the $f$-electron self-energy function near the Fermi level. The following values of the parameters are used: $\tilde{E}_0/\xi_{p_F}=-0.003$, $V/\xi_{p_F}=0.02$, $U\rho_s(\xi_{p_F})=0.1$, and $D/\xi_{p_F}=1.5$.

we have

$$\mathrm{Im}\Sigma(p_0,\mathbf{p}) \sim -\frac{\lambda_r^2}{2}\int \frac{d^3k}{(2\pi)^3}\frac{d^3q}{(2\pi)^3}\left[U\chi_s - \frac{V^2(\varepsilon_{\mathbf{k}+\mathbf{q}}-\varepsilon_{\mathbf{k}})}{\varepsilon_{\mathbf{k}}\varepsilon_{\mathbf{k}+\mathbf{q}}}\right] \times\rho_0(0,\mathbf{p}+\mathbf{q})\rho_0(0,\mathbf{k})\rho_0(0,\mathbf{k}+\mathbf{q})p_0^2\mathrm{sgn}(p_0)\,, \tag{3.39}$$

for $p_0\sim 0$. We also see in Fig. 5 that the imaginary part of the self-energy has a large peak below the Fermi level. Using this self-energy function, we calculated the spectral function of the $f$-electron Green's function near the Fermi level for several values of the momentum. The result is presented in Fig. 6. The spectral function near the Fermi level has one sharp peak in the energy domain very close to the Fermi level and a broad resonance peak above the sharp peak. The sharp peak corresponds to the quasiparticle excitation in our Anderson lattice system since the lifetime of the excitation with the Fermi momentum is infinitely long [Fig. 6(b)]. Therefore the Anderson lattice behaves as a Fermi liquid. The resonance peak lying above the quasiparticle states originate from the many-body interaction and is similar to the resonance peak seen in the Kondo regime of the single-impurity Anderson model. To understand the nature of the excitation we plot the real part of the inverse $f$-electron Green's function

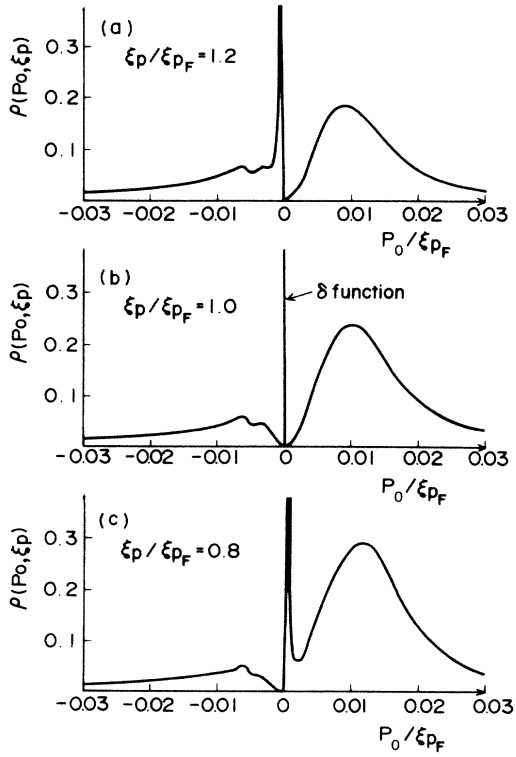


FIG. 6. Energy dependence of the $f$-electron spectral function near the Fermi level. The following values of the parameters are used: $\tilde{E}_0/\xi_{p_F}=-0.003$, $V/\xi_{p_F}=0.02$, $U\rho_{p_F}(\xi_{p_F})=0.1$, and $D/\xi_{p_F}=1.5$.

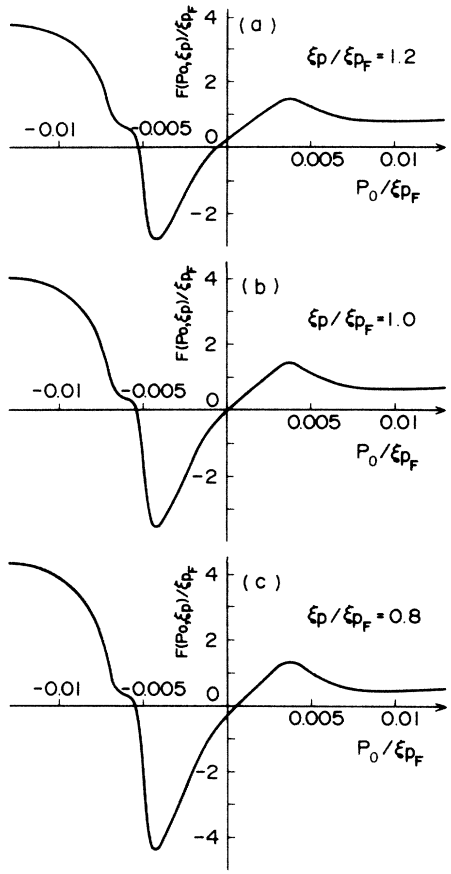


FIG. 7. Energy dependence of the real part of the inverse $f$-electron Green's function near the Fermi level. The following values of the parameters are used: $\tilde{E}_0/\xi_{p_F}=-0.003$, $V/\xi_{p_F}=0.02$, $U\rho_s(\xi_{p_F})=0.1$, and $D/\xi_{p_F}=1.5$.

$$F(p_0,\xi_p)\equiv \mathrm{Re}g^{-1}(p_0,\xi_p) = p_0-\tilde{E}_0-\frac{V^2}{p_0-\varepsilon_p}-\mathrm{Re}\tilde{\Sigma}(p_0,\xi_p)\,, \tag{3.40}$$

as a function of the energy $p_0$ for fixed $\xi_p$ in Fig. 7. Here

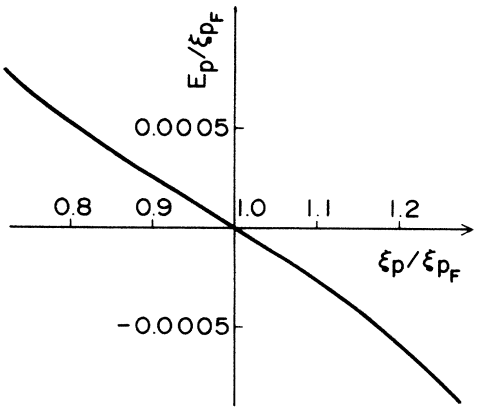


FIG. 8. Energy spectrum of the quasiparticle. The following values of the parameters are used: $\tilde{E}_0/\xi_{p_F}=-0.003$, $V/\xi_{p_F}=0.02$, $U\rho_s(\xi_{p_F})=0.1$, and $D/\xi_{p_F}=1.5$.

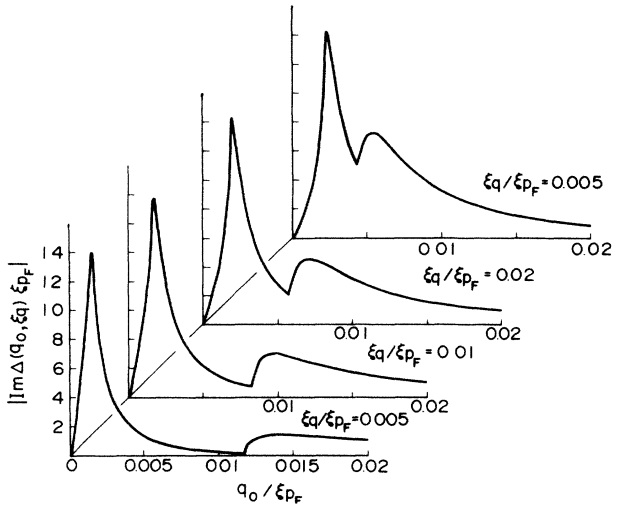


FIG. 9. Energy dependence of the imaginary part of the spin-fluctuation Green's function. The following values of the parameters are used: $\tilde{E}_0/\xi_{p_F}=0.003$, $V/\xi_{p_F}=0.02$, $U\rho_s(\xi_{p_F})=0.1$, and $D/\xi_{p_F}=1.5$.

the last term $\mathrm{Re}\tilde{\Sigma}(p_0,\xi_p)$ is calculated by using the relation (3.10). Note that the zero points of this function give the stable single-particle excitation energy if the imaginary part of the self-energy is infinitesimal. As seen in Fig. 7, the function (3.40) has two zero points. The zero point being closer to the Fermi level gives the single-particle state seen in the spectral function of the $f$-electron Green's function (see Fig. 6). When the zero point appears at $p_0=0$, the single-particle excitation is perfectly stable, because the imaginary part of the self-energy is infinitesimal. On the other hand, the other zero point which is apart from the Fermi level does not give a single-particle-like excitation, since the imaginary part of the self-energy is quite large at this energy as seen in Fig. 5. The resonance peak at $p_0/\xi_{p_F}\sim 0.01$ in Fig. 6 comes from both the real part (3.40) and the imaginary part of the self-energy being small in that energy range. In Fig. 8 we show the energy spectrum $E_p$ of the single-particle states as a function of $\xi_p/\xi_{p_F}$. In this selection of the parameters we have a holelike excitation spectrum. The effective mass $m^*$ of the quasiparticle in our Anderson-lattice system can be obtained from the relation

$$m^*/m=1\Big/\left[\frac{\partial E_p}{\partial \xi_p}\right]_{p_F}. \tag{3.41}$$

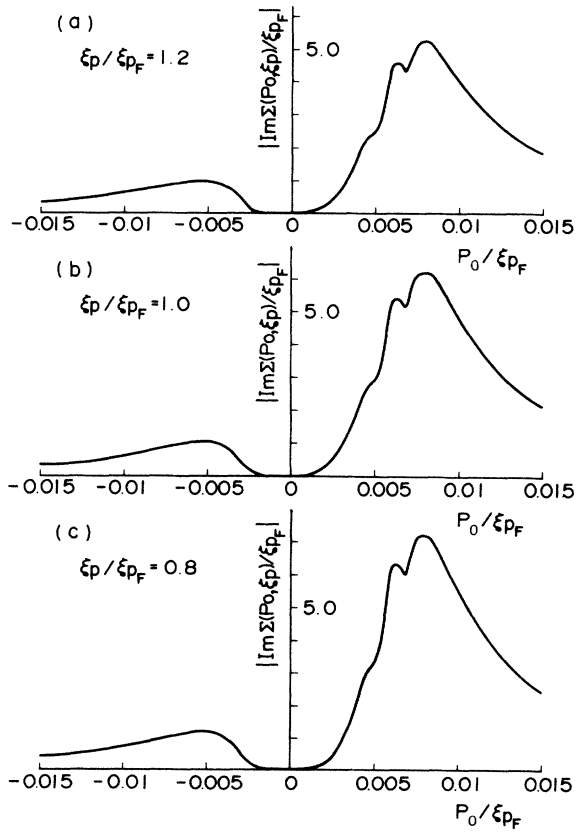


FIG. 10. Energy dependence of the imaginary part of the $f$-electron self-energy function near the Fermi level. The following values of the parameters are used: $\tilde{E}_0/\xi_{p_F}=0.003$, $V/\xi_{p_F}=0.02$, $U\rho_s(\xi_{p_F})=0.1$, and $D/\xi_{p_F}=1.5$.

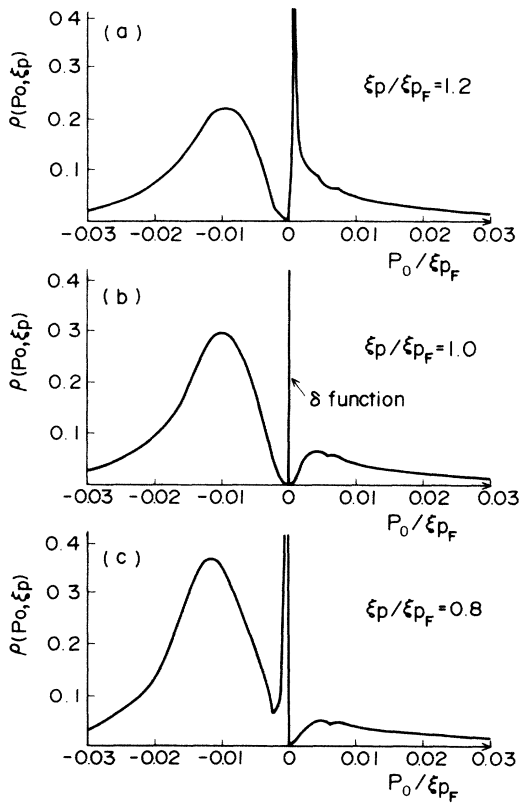


FIG. 11. Energy dependence of the $f$-electron spectral function near the Fermi level. The following values of the parameters are used: $\tilde{E}_0/\xi_{p_F}=0.003$, $V/\xi_{p_F}=0.02$, $U\rho_s(\xi_{p_F})=0.1$, and $D/\xi_{p_F}=1.5$.

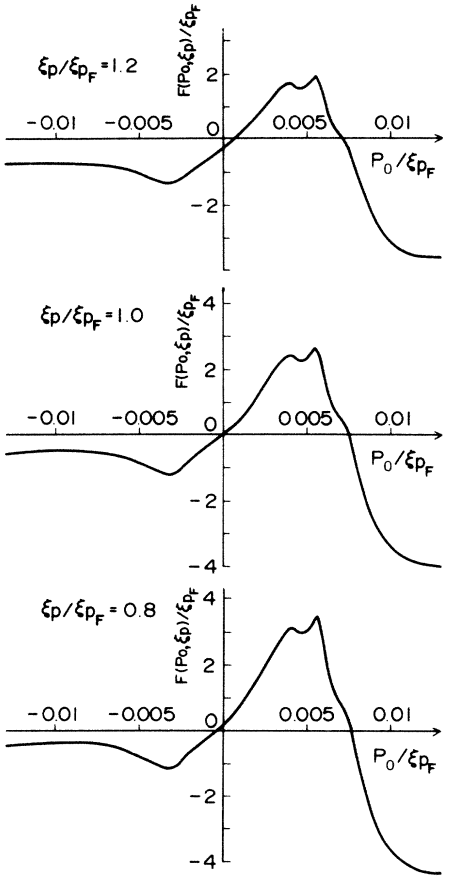


FIG. 12. Energy dependence of the real part of the inverse $f$-electron Green's function near the Fermi level. The following values of the parameters are used: $\tilde{E}_0/\xi_{p_F}=0.003$, $V/\xi_{p_F}=0.02$, $U\rho_s(\xi_{p_F})=0.1$, and $D/\xi_{p_F}=1.5$.

Using the results given in Fig. 8 for the relation (3.41), we obtain the mass ratio $|m^*/m| \sim 400$. Thus, we see that a fermion state with quite heavy mass is realized in the Anderson-lattice system.

In Figs. 9—13 we show the results from a selection of the values of the parameters $\tilde{E}_0/\xi_{p_F}=0.003$, $V/\xi_{p_F}=0.02$, $U\rho_s(\varepsilon_F)=0.1$, and $D/\xi_{p_F}=1.5$. In this case we chose $\tilde{E}_0$ to be positive. These results are qualitatively the same as the previous ones. A difference lies in the peak position in the imaginary part of the self-energy. That is, the large peak appears above the Fermi level in contrast with the previous case as seen in Fig. 10. Whether the peak is situated above or below the Fermi level depends on the sign of $\tilde{E}_0$. In this selection of the values of the parameters, a broader resonance peak appears below the Fermi level (Fig. 11). The dispersion of the quasiparticle energy is shown in Fig. 13, which is obtained from the zero points of the function illustrated in Fig. 12. In this case we find a particlelike excitation spectrum with the mass ratio $m^*/m \sim 290$.

Figures 14 and 15 show the results when we take a much smaller value of $\tilde{E}_0$, i.e., $\tilde{E}_0/\xi_{p_F}=0.0015$, keeping

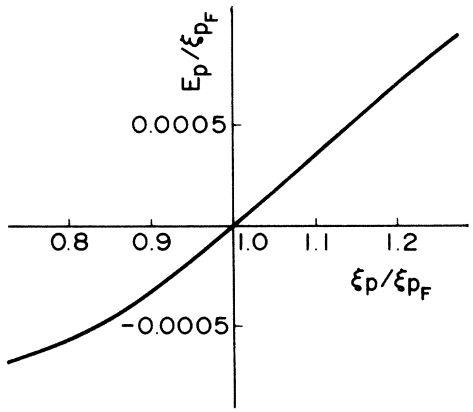


FIG. 13. Energy spectrum of the quasiparticle. The following values of the parameters are used: $\tilde{E}_0/\xi_{p_F}=0.003$, $V/\xi_{p_F}=0.02$, $U\rho_s(\xi_{p_F})=0.1$, and $D/\xi_{p_F}=1.5$.

the other parameters unchanged. In Fig. 14 we see that spectral function is sharpened more and the resonance peak is much more narrow compared with the previous cases. The effective mass ratio of the quasiparticle obtained from the energy spectrum shown in Fig. 15 is $m^*/m \sim 1100$.

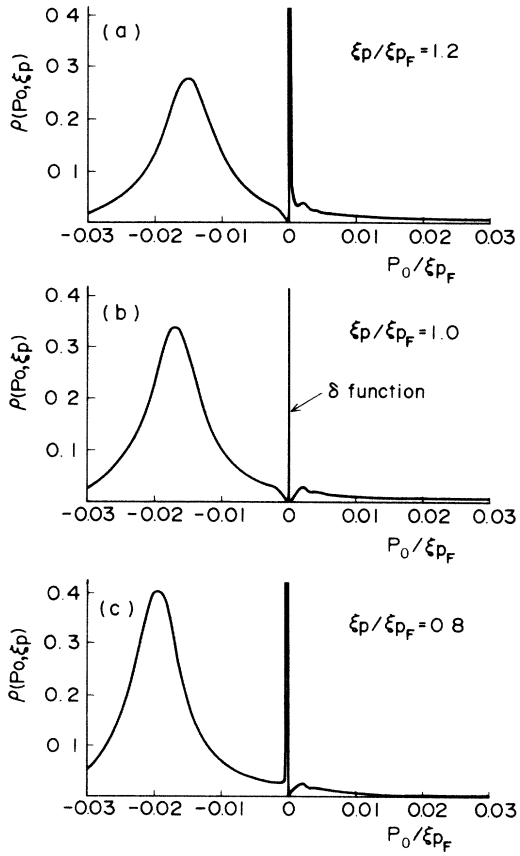


FIG. 14. Energy dependence of the $f$-electron spectral function near the Fermi level. The following values of the parameters are used: $\tilde{E}_0/\xi_{p_F}=0.0015$, $V/\xi_{p_F}=0.02$, $U\rho_s(\xi_{p_F})=0.1$, and $D/\xi_{p_F}=1.5$.

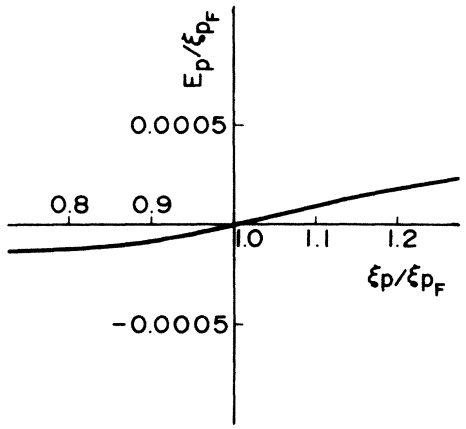


FIG. 15. Energy spectrum of the quasiparticle. The following values of the parameters are used: $\tilde{E}_0/\xi_{p_F}=0.0015$, $V/\xi_{p_F}=0.02$, $U\rho_s(\xi_{p_F})=0.1$, and $D/\xi_{p_F}=1.5$.

## IV. DISCUSSION AND SUMMARY

In the present paper we investigated the low-energy properties in the Anderson-lattice system by making a one-loop correction due to the spin fluctuations to the $f$-electron self-energy at $T=0$ K. The formulation presented here is also applicable to the single-impurity Anderson model. In the single-impurity Kondo case, our theory which includes the one-loop approximation satisfies the exact relations among the self-energy, the vertex functions, and the susceptibility,[29–33] and leads to the correct feature of the resonance state around the Fermi level.[34] Therefore, we consider that this approach is also suitable for treating the Anderson-lattice system. We believe that the result obtained in this paper does correctly delineate the behavior of the low-energy excitations in the Anderson lattice.

We found that the low-energy excited states in the Anderson lattice-system are composed of both a quasiparticle state with heavy mass and a many-body resonance state when the renormalized $f$-level parameter $\tilde{E}_0$ is close to the Fermi level. In the single-Kondo-impurity system, as is well known, the resonance state appears just around the Fermi level below the Kondo temperature. However, no stable quasiparticle state exists because of the lack of the translational symmetry. Thus the features of the excitation in the Anderson lattice clearly differ from those in the single-impurity system on the point that the well-defined quasiparticle state exists just around the Fermi level. Therefore, the heavy fermion state in the cerium and uranium compounds may be identified with the quasiparticle state obtained in the present calculation. The large electronic specific heat observed in the heavy Fermion compounds such as $CeCu_2Si_2$, $CeAl_3$, and $CeCu_6$ is attributed to this quasiparticle excitation.

The nature of the quasi-fermion state can be explained in the following way. We suppose a quantum-mechanical superposition of the $f$-electron states of up and down spins. Then the level of this $f$-electron state is lifted up near to the Fermi level due to the correlation interaction acting between the $f$ electrons with up and down spins.

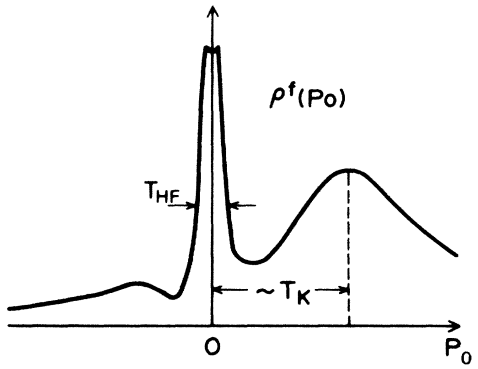


FIG. 16. Schematic representation of the $f$-electron density of states near the Fermi level at $T=0$ K.

The $f$-electron state at each lattice site is partially hybridized with the conduction-electron state by the conduction-electron–$f$-electron mixing interaction. This hybridized state is a Fermi liquid state near the Fermi level. The mass of the Fermi liquid is strongly enhanced by the renormalization effect due to the spin fluctuations. Accordingly, the heavy fermions in the Fermi liquid state are the conduction-electron–$f$-electron hybridized electrons which are heavily dressed by the spin-fluctuation cloud.

It is noted that the width of the quasiparticle band is very narrow compared with that of resonance level as seen from the $f$-electron spectral functions obtained in Sec. III. The density of states of $f$ electrons is obtained by summing the spectral function (3.57) over the entire **p** space. However, the accurate evaluation of the density of states is quite difficult owing to the singular behavior of the spectral function around the Fermi level. Therefore, we illustrate the density of states schematically in Fig. 16. As shown in this figure we expect to have two characteristic energy scales $T_{HF}$ and $T_k$, which correspond, respectively, to the heavy-fermion band width and the energy of the resonance peak position. We suppose that $T_{HF}$ takes a few Kelvin in typical heavy-fermion systems. The other energy scale $T_k$ is similar to the Kondo temperature in the single-impurity case. The values of $T_{HF}$ is almost 1

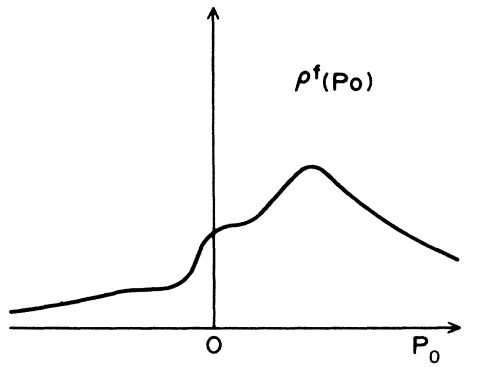


FIG. 17. Schematic representation of the $f$-electron density of states near the Fermi level at a temperature between $T_{HF}$ and $T_k$.

order of magnitude smaller than $T_k$.

Our theory presented in this paper is restricted to absolute zero. Now we are extending our theory to finite temperatures and planning to calculate the specific heat and the electrical resistivity at finite temperatures. For the present, we may speculate the temperature variation of the state in the Anderson lattice on the basis of the above picture for the energy excitation. At finite temperatures the thermal fluctuations lead to a finite value of the imaginary part of the self-energy even for $p_0=0$. As temperature increases above $T_{\rm HF}$ the imaginary part increases and then the quasiparticle state cannot be well defined anymore. In the temperature range, $T_{\rm HF}<T<T_k$, thus, we expect only the resonance peak in the $f$-electron density of states near the Fermi level as shown schematically in Fig. 17. This structure change of the density of states indicates the occurrence of the crossover behavior from the heavy-fermion state to the single-impurity-like resonance state seen in the heavy-fermion compounds.

Finally, we briefly discuss the experimental results for the specific heat in the heavy-fermion compounds. In the compounds such as $CeCu_2Si_2$, $CeAl_3$, and $CeCu_6$ the quantity of the specific heat divided by temperature $C/T$ has extremely large values below 1 K. In $CeCu_6$, it has been observed that an application of magnetic fields of several Teslas strongly depresses the quantity $C/T$ below 1 K.[35] The temperature and field dependences are consistent with the present theoretical result that a narrow quasifermion band exists near the Fermi level only at very low temperatures. In some of the heavy-fermion compounds the quantity $C/T$ has a maximum below 1 K. The appearance of the maximum may result from fine structure in the density of states of the quasiparticles.


## ACKNOWLEDGMENT

This work has been supported by a Grant-in-Aid from the Ministry of Education, Science and Culture, Japan.


## APPENDIX

In this appendix we make the momentum integrations given in Sec. III using the new variables $\xi_p$ and $\Theta$,

$$\int \frac{d^3p}{(2\pi)^3}(\cdots)=\rho_s(\xi_{p_F})\int_0^D d\xi_p(\xi_p/\xi_{p_F})^{1/2} \times\tfrac{1}{2}\int_{-1}^{1} d(\cos\theta)(\cdots)\,, \tag{A1}$$

$\rho_s(p_F)$ being the density of states of the bare conduction band with band width $D$ at $\xi_p=\xi_{p_F}$, i.e.,

$$\rho_s(\xi_{p_F})=(2m^3)^{1/2}\xi_{p_F}^{1/2}/(2\pi)^2\,. \tag{A2}$$

Using (A1) for (3.25)–(3.28), we can perform the integrations by $\cos\Theta$ and have the result for the spectral function of the spin-fluctuation Green's function,

$$D(q_0,\mathbf{q})\equiv D(q_0,\xi_q) =\frac{\rho_s(\xi_{p_F})}{2(\xi_q\xi_{p_F})^{1/2}}[\tilde{D}_1(q_0,\xi_q)+\tilde{D}_2(q_0,\xi_q) +\tilde{D}_3(q_0,\xi_q)+\tilde{D}_4(q_0,\xi_q)]\,, \tag{A3}$$

where

$$\tilde{D}_1(q_0,\xi_q)=\int_{c_1} d\xi_p \left[U\chi_s-\frac{V^2[\tilde{E}_0-\varepsilon_p+B(\varepsilon_p)]}{[q_0+A_+(\varepsilon_p)-\varepsilon_p-X(q_0,\varepsilon_p)][A_+(\varepsilon_p)-\varepsilon_p][2q_0+B(\varepsilon_p)-\tilde{E}_0+\varepsilon_p]}\right] \times\frac{|\,q_0+A_+(\varepsilon_p)-\varepsilon_p-X(q_0,\varepsilon_p)\,|\;|\,A_+(\varepsilon_p)-\varepsilon_p\,|\,[\Theta(A_+(\varepsilon_p))-\Theta(q_0+A_+(\varepsilon_p))]}{B(\varepsilon_p)\,|\,X(q_0,\varepsilon_p)-\tilde{E}_0+\varepsilon_p+[B(\varepsilon_p)^2-2(\tilde{E}_0-\varepsilon_p)X(q_0,\varepsilon_p)+X(q_0,\varepsilon_p)^2]^{1/2}\,|} \tag{A4}$$

$$\tilde{D}_2(q_0,\xi_q)=\int_{c_2} d\xi_p \left[U\chi_s-\frac{V^2[\tilde{E}_0-\varepsilon_p+B(\varepsilon_p)]}{[q_0+A_+(\varepsilon_p)-\varepsilon_p-X(q_0,\varepsilon_p)][A_+(\varepsilon_p)-\varepsilon_p][2q_0+B(\varepsilon_p)-\tilde{E}_0+\varepsilon_p]}\right] \times\frac{|\,q_0+A_+(\varepsilon_p)-\varepsilon_p-X(q_0,\varepsilon_p)\,|\;|\,A_+(\varepsilon_p)-\varepsilon_p\,|\,[\Theta(A_+(\varepsilon_p))-\Theta(q_0+A_+(\varepsilon_p))]}{B(\varepsilon_p)\,|\,X(q_0,\varepsilon_p)-\tilde{E}_0+\varepsilon_p-[B(\varepsilon_p)^2-2(\tilde{E}_0-\varepsilon_p)X(q_0,\varepsilon_p)+X(q_0,\varepsilon_p)^2]^{1/2}\,|}\,, \tag{A5}$$

$$\tilde{D}_3(q_0,\xi_q)=\int_{c_3} d\xi_p \left[U\chi_s-\frac{V^2[\tilde{E}_0-\varepsilon_p-B(\varepsilon_p)]}{[q_0+A_-(\varepsilon_p)-\varepsilon_p-\bar{X}(q_0,\varepsilon_p)][A_-(\varepsilon_p)-\varepsilon_p][2q_0-B(\varepsilon_p)-\tilde{E}_0+\varepsilon_p]}\right] \times\frac{|\,q_0+A_-(\varepsilon_p)-\varepsilon_p-\bar{X}(q_0,\varepsilon_p)\,|\;|\,A_-(\varepsilon_p)-\varepsilon_p\,|\,[\Theta(A_-(\varepsilon_p))-\Theta(q_0+A_-(\varepsilon_p))]}{B(\varepsilon_p)\,|\,\bar{X}(q_0,\varepsilon_p)-\tilde{E}_0+\varepsilon_p+[B(\varepsilon_p)^2-2(\tilde{E}_0-\varepsilon_p)\bar{X}(q_0,\varepsilon_p)+\bar{X}(q_0,\varepsilon_p)^2]^{1/2}\,|}\,, \tag{A6}$$

$$\tilde{D}_4(q_0,\xi_q)=\int_{c_4} d\xi_p \left[ U\chi_s - \frac{V^2[\tilde{E}_0-\varepsilon_p-B(\varepsilon_p)]}{[q_0+A_-(\varepsilon_p)-\varepsilon_p-\bar{X}(q_0,\varepsilon_p)][A_-(\varepsilon_p)-\varepsilon_p][2q_0-B(\varepsilon_p)-\tilde{E}_0+\varepsilon_p]} \right]$$

$$\times \frac{|\,q_0+A_-(\varepsilon_p)-\varepsilon_p-\bar{X}(q_0,\varepsilon_p)\,|\;|\,A_-(\varepsilon_p)-\varepsilon_p\,|\,[\Theta(A_-(\varepsilon_p))-\Theta(q_0+A_-(\varepsilon_p))]}{B(\varepsilon_p)\,|\,\bar{X}(q_0,\varepsilon_p)-\tilde{E}_0+\varepsilon_p-[B(\varepsilon_p)^2-2(\tilde{E}_0-\varepsilon_p)\bar{X}(q_0,\varepsilon_p)+\bar{X}(q_0,\varepsilon_p)^2]^{1/2}\,|} , \tag{A7}$$

where

$$X(q_0,\varepsilon_p)=\frac{q_0[B(\varepsilon_p)+\tilde{E}_0-\varepsilon_p]}{[2q_0+B(\varepsilon_p)-\tilde{E}_0+\varepsilon_p]} , \tag{A8}$$

$$\bar{X}(q_0,\varepsilon_p)=\frac{q_0[\tilde{E}_0-\varepsilon_p-B(\varepsilon_p)]}{[2q_0-B(\varepsilon_p)-\tilde{E}_0+\varepsilon_p]} . \tag{A9}$$

The integral domains $c_1$–$c_4$, are taken in such a way that the integration variable $\xi_p$ satisfies the conditions

$$X(q_0,\varepsilon_p)\le 2q_0+B(\varepsilon_p)$$

and (A10)

$$\xi_q-2\xi_p^{1/2}\xi_q^{1/2}\le X(q_0,\varepsilon_p)\le\xi_q+2\xi_p^{1/2}\xi_q^{1/2} \quad \text{for } c_1 ;$$

$$X(q_0,\varepsilon_p)\ge 2q_0+B(\varepsilon_p)$$

and (A11)

$$\xi_q-2\xi_p^{1/2}\xi_q^{1/2}\le X(q_0,\varepsilon_p)\le\xi_q+2\xi_p^{1/2}\xi_q^{1/2} \quad \text{for } c_2 ;$$

$$\bar{X}(q_0,\varepsilon_p)\le 2q_0-B(\varepsilon_p)$$

and (A12)

$$\xi_q-2\xi_p^{1/2}\xi_q^{1/2}\le \bar{X}(q_0,\varepsilon_p)\le\xi_q+2\xi_p^{1/2}\xi_q^{1/2} \quad \text{for } c_3 ;$$

$$\bar{X}(q_0,\varepsilon_p)\ge 2q_0-B(\varepsilon_p)$$

and (A13)

$$\xi_q-2\xi_p^{1/2}\xi_q^{1/2}\le \bar{X}(q_0,\varepsilon_p)\le\xi_q+2\xi_p^{1/2}\xi_q^{1/2} \quad \text{for } c_4 .$$

Let us next calculate the susceptibility $\chi_s$ in the integrands in Eqs. (3.25)–(3.28). The equation for $\chi_s$ is given from Eq. (2.32) and the Ward-Takahashi relation (2.39) in the limit $h_s\to 0$ by

$$\chi_s=V^2\frac{i}{(2\pi)^4}\int d^4p\frac{V^2}{(p_0-\varepsilon_p)^2}\left[1-2\left[\frac{\partial\Sigma_\uparrow(p)}{\partial h_f}\right]_{h=0}\right]$$

$$\times g_\downarrow(p)g_\uparrow(p) . \tag{A14}$$

When the approximate spectral function (3.12) is used, we find

$$\left[\frac{\partial\Sigma_\uparrow(p)}{\partial h_f}\right]_{h=0}=\tfrac{1}{2}U\Delta(0)\equiv\tfrac{1}{2}U\chi_f . \tag{A15}$$

Then, Eq. (A14) leads to

$$\chi_s=R(1-U\chi_f) , \tag{A16}$$

with

$$R=\frac{i}{(2\pi)^4}\int d^4p\frac{V^2}{(p_0-\varepsilon_p)^2}g_\downarrow(p)g_\uparrow(p)$$

$$=V^2\rho_s(\xi_{p_F})/(\tilde{E}_0^2+V^2) . \tag{A17}$$

On the other hand $\chi_f$ can be obtained from Eq. (2.47) in the limit $q_0\to 0$, $\bar{q}\to\mathbf{0}$ as

$$\chi_f\equiv\Delta(0)=R-U\chi_sQ , \tag{A18}$$

with

$$Q=\frac{i}{(2\pi)^4}\int d^4p\, g_\uparrow(p)g_\downarrow(p)$$

$$=V^4\rho_s(\xi_{p_F})/[\tilde{E}_0^2(\tilde{E}_0^2+V^2)] . \tag{A19}$$

From Eqs. (A16) and (A18), we obtain

$$\chi_s=R(1-UQ)/(1-U^2QR) , \tag{A20}$$

$$\chi_f=R(1-UR)/(1-U^2QR) . \tag{A21}$$

The imaginary part of the $f$-electron self-energy can be calculated by substituting the above results for $D(q_0,\xi_q)$, Eqs. (A3) and (3.12) into Eq. (3.5). The integration by $q_0$ in Eq. (3.5) can be performed in the same way as in the above calculation for the spectral function $D(q_0,\xi_q)$. The result for $\tilde{\Sigma}_2(p_0,\xi_p)$ is given by

$$\tilde{\Sigma}_2(p_0,\xi_p)=\{[\lambda_r\rho_s(\xi_{p_F})]^2/(2\xi_{p_F}^{1/2})\}\int_0^D d\xi_k\frac{\xi_k^{1/2}}{B(\varepsilon_k)}\,|\,A_+(\varepsilon_k)-\varepsilon_k\,|\,[\Theta(A_+(\varepsilon_k)-p_0)-\Theta(A_+(\varepsilon_k))]$$

$$\times\int_{-1}^{1}dt\tilde{D}(A_+(\varepsilon_k)-p_0,\xi_k+\xi_p-2\xi_k^{1/2}\xi_p^{1/2}t)$$

$$+\{[\lambda_r\rho_s(\varepsilon_{p_F})]^2/(2\xi_{p_F}^{1/2})\}\int_0^D d\xi_k\frac{\xi_k^{1/2}}{B(\varepsilon_k)}\,|\,A_-(\varepsilon_k)-\varepsilon_k\,|\,[\Theta(A_-(\varepsilon_k)-p_0)-\Theta(A_-(\varepsilon_k]$$

$$\times\int_{-1}^{1}dt\,\tilde{D}(A_-(\varepsilon_k)-p_0,\xi_k+\xi_p-2\xi_k^{1/2}\xi_p^{1/2}t) . \tag{A22}$$

[1]For experimental results see, for example, G. R. Steward, Rev. Mod. Phys. **56**, 755 (1984).
[2]Y. Ōnuki, Y. Shimizu, and T. Komatsubara, J. Phys. Soc. Jpn. **53**, 1210 (1984).
[3]G. R. Stewart, Z. Fisk, and M. S. Wire, Phys. Rev. B **30**, 482 (1984).
[4]A. Benoit, A. Barton, J. Chaussy, J. Flouquet, J. C. Lasjaunias, J. Odin, J. Palleau, J. Peyrard, and M. Ribault, in *Valence Fluctuations in Solids,* edited by L. M. Falicov, W. Hanke, and M. B. Maple (North-Holland, Amsterdam, 1981), p. 298.
[5]F. Steglich, J. Aarts, C. D. Bredl, W. Lieke, D. Meschede, W. Franz, and J. Schafer, Phys. Rev. Lett. **43**, 1892 (1979).
[6]A. Yoshimori and H. Kasai, J. Magn. Magn. Mater. **31-34**, 475 (1983).
[7]F. J. Ohkawa, J. Phys. Soc. Jpn **52**, 3886 (1983).
[8]M. Tachiki and S. Maekawa, Phys. Rev. B **29**, 2497 (1984).
[9]H. Razafimandimby, P. Fulde, and J. Keller, Z. Phys. B **54**, 111 (1984).
[10]N. d'Ambramenil and P. Fulde, in *Theory of Heavy Fermions and Valence Fluctuations,* edited by T. Kasuya and T. Saso (Springer-Verlag, 1985), p. 195.
[11]P. Coleman, Phys. Rev. B **29**, 3035 (1984); in *Theory of Heavy Fermions and Valence Fluctuations,* Ref. 10, p. 163
[12]D. Newns and N. Read, J. Phys. C **16**, L1055 (1983).
[13]D. Newns, N. Read, and A. Hewson, in *Moment Formation in Solids,* edited by W. L. Buyers (Plenum, New York, 1984), p. 257.
[14]C. M. Varma, in *Theory of Heavy Fermions and Valence Fluctuations,* Ref. 10, p. 83.
[15]B. H. Brandow, Phys. Rev. B **33**, 215 (1985).
[16]K. Ueda and T. M. Rice, Phys. Rev. Lett. **55**, 995 (1985).
[17]Y. Kuramoto and C. Horie, J. Magn. Magn. Mater. **47-48**, 343 (1985); Y. Kuramoto, in *Theory of Heavy Fermions and Valence Fluctuations,* Ref. 10, p. 152.
[18]H. Grewe, Solid State Commun. **50**, 19 (1984).
[19]R. M. Martin and J. W. Allen, J. Appl. Phys. **50**, 7561 (1979).
[20]H. Matsumoto and H. Umezawa, Phys. Rev. B **31**, 4433 (1985).
[21]H. Fukuyama, in *Theory of Heavy Fermions and Valence Fluctuations,* Ref. 10, p. 152.
[22]K. Yamada and K. Yosida, in *Theory of Heavy Fermions and Valence Fluctuations,* Ref. 10, p. 183.
[23]The vertex functions $\Gamma_+(p;q;r)$ and $\Gamma_-(p;q;r)$ are not independent of each other. Using the relation (2.12), we can obtain the equation for the spin-fluctuation Green's function,

$$\Delta(q)=-\frac{i}{(2\pi)^4}\int_c d^4p\, g_\uparrow(p)g_\downarrow(p+q)$$
$$+\frac{i}{(2\pi)^4}\int_c d^4p\,\Delta(q)\Gamma_-(p+q;q;p)$$
$$\times g_\uparrow(p)g_\downarrow(p+q)\,.$$

Comparing this equation with Eq. (2.18), we find the relation

$$\Gamma_+(p;q;p+q)=\Gamma_-(p+q;q;p)\,.$$

[24]H. Umezawa, H. Matsumoto, and M. Tachiki, in *Thermo Field Dynamics and Condensed States* (North-Holland, Amsterdam, 1982), Chap. 6.
[25]H. Matsumoto, H. Umezawa, S. Seki, and M. Tachiki, Phys. Rev. B **17**, 2276 (1977).
[26]J. A. Hertz and D. M. Edwards, J. Phys. F **3**, 2174 (1974).
[27]U. Brandt, W. Pesch, and L. Tewort, Z. Phys. **238**, 121 (1970).
[28]J. Whitehead, H. Matsumoto, and H. Umezawa, Phys. Rev. B **25**, 4737 (1982).
[29]T. Koyama and M. Tachiki, Prog. Theor. Phys. Suppl. **80**, 108 (1984).
[30]K. Yamada, Prog. Theor. Phys. **53**, 967 (1975).
[31]K. Yosida and K. Yamada, Prog. Theor. Phys. **53**, 1286 (1975).
[32]H. Shiba, Prog. Theor. Phys. **54**, 967 (1975).
[33]A. Yoshimori, Prog. Theor. Phys. **55**, 67 (1976).
[34]T. Koyama and M. Tachiki (unpublished).
[35]K. Satoh, T. Fujita, Y. Maeno, Y. Ōnuki, T. Komatsubara, and T. Ohtsuka, Solid State Commun. **56**, 327 (1985).